

Growth and life habits of the Triassic cynodont *Trirachodon*, inferred from bone histology

JENNIFER BOTHA and ANUSUYA CHINSAMY



Botha, J. and Chinsamy, A. 2004. Growth and life habits of the Triassic cynodont *Trirachodon*, inferred from bone histology. *Acta Palaeontologica Polonica* 49 (4): 619–627.

Growth pattern and lifestyle habits of the Triassic non-mammalian cynodont *Trirachodon* are deduced from bone histology and cross-sectional geometry. Several skeletal elements of *Trirachodon* were examined in order to document histological changes during ontogeny, as well as histovariability in the skeleton. The bone histology of all the elements consists of a moderately vascularized, periodically interrupted, fibro-lamellar bone tissue. This suggests that the overall growth of *Trirachodon* was probably rapid during the favourable season, but decreased or ceased during the unfavourable season. As the environment is thought to have been semi-arid with seasonal rainfall, it is possible that *Trirachodon* was sensitive to such environmental fluctuations. Some inter-elemental histovariability was noted where the number and prominence of growth rings varied. Limb bone cross-sectional geometry revealed a relatively thick bone wall and supports earlier proposals that *Trirachodon* was fossorial.

Key words: Cynodonts, *Trirachodon*, lifestyles, bone histology, growth patterns.

Jennifer Botha [jbotha@iziko.org.za], Natural History Collections Division, South African Museum, Iziko Museums of Cape Town, P.O. Box 61, 8000, South Africa (corresponding author);

Anusuya Chinsamy [achinsam@botzoo.uct.ac.za], Zoology Department, University of Cape Town, Rondebosch, 7701, South Africa.

Introduction

Trirachodon is a herbivorous non-mammalian cynodont whose remains have been found in the Early to Middle Triassic *Cynognathus* Assemblage Zone, of the Beaufort Group, Karoo Supergroup of South Africa (Rubidge 1995). The cranium of *Trirachodon* is similar to *Diademodon*, a contemporary non-mammalian cynodont, and is characterized by a short, narrow snout; wide orbital region; slender zygomatic arches and antero-dorsally placed eyes (Seeley 1895a; Kemp 1982). However, *Trirachodon*, with a maximum body length of 50 cm, is much smaller than the 2 m long *Diademodon* and has fewer gomphodont (molariform) postcanine teeth, which are broader transversely and anteroposteriorly shorter than those of *Diademodon* (Seeley 1895b; Crompton and Ellenberger 1957; Kemp 1982).

Trirachodon had a more mammal-like posture than the earlier, more basal cynodont genera such as the Permian *Procynosuchus*. In *Trirachodon* though, the forelimb still had a sprawling orientation (Kemp 1982). The hindlimb posture was semi-erect (Kemp 1982), which would have improved the locomotor efficiency of the animal, possibly allowing for more sustained activity (Carrier 1987; Pough et al. 1996). Other derived mammalian characteristics include a bony secondary palate and precise postcanine tooth occlusion, both of which would have increased food-processing efficiency (Kemp 1982). Compared to other non-mammalian cynodonts, *Trirachodon* fossils are relatively scarce and the

few studies that have examined *Trirachodon* have focused on its morphology (Seeley 1895b; Crompton and Ellenberger 1957; Kemp 1982), which has led to a rather limited understanding of its biology.

Given that bone histology is well recognized as providing pertinent information about the biology of extinct vertebrates (e.g., Amprino 1947; Ricqlès 1969, 1972, 1974, 1976, 1980; Chinsamy 1990, 1993a, 1995, 1997; Reid 1996; Horner et al. 2000; Ricqlès et al. 2001, 2003), we applied this methodology to *Trirachodon*. Although the organic components of bone (which include osteocytes, vascular canals and collagenous fibres) are destroyed during fossilization, their structural organization usually remains intact, thereby allowing the bone tissue microstructure of the fossil to be discerned (Francillon-Vieillot et al. 1990). Comparing the bone microstructure with that of living animals allows various aspects such as growth, individual age and the lifestyle habits of extinct animals to be interpreted (e.g., Enlow and Brown 1956, 1957). Several early bone microstructure studies on isolated skeletal remains of non-mammalian therapsids have been conducted (e.g., Enlow and Brown 1956, 1957). However, in the late 1960s and 1970s Armand de Ricqlès undertook a systematic assessment of the bone microstructure of a variety of non-mammalian therapsids including dinocephalians and dicynodonts (Ricqlès 1972), and therocephalians, gorgonopsians, and cynodonts (Ricqlès 1969). Although his analyses were mainly on isolated fragments of specimens identified only to generic level, they nevertheless provided an impor-

tant understanding of the range of bone tissue types present among the non-mammalian therapsids. Until now, however, *Trirachodon* has yet to be studied.

It has previously been suggested that *Trirachodon* was a fossorial animal, based on skeletal remains preserved inside burrow casts recovered from the Driekoppen Formation in South Africa (Groenewald et al. 2001) and the Omingonde Formation in Namibia (Smith and Swart 2002). As studies on the cross-sectional geometry of bone have shown that a direct relationship exists between an animal's lifestyle and the structural design of its bones (Wall 1983; Stein 1989; Fish 1993; Bou et al. 1990), here we combine the histological analysis with an assessment of the cross-sectional geometry of *Trirachodon* limb bones.

Institutional abbreviations.—NMQR, National Museum, Bloemfontein; SAM-PK, South African Museum, Iziko Museums of Cape Town; CGP, Council for Geoscience, Pretoria.

Materials and methods

Trirachodon remains have been recovered from the *Cynognathus* Assemblage Zone, of the Beaufort Group, Karoo Supergroup of South Africa (Rubidge 1995), and are currently housed in various institutions in South Africa. For our analysis, eleven skeletal elements, including femora, tibiae, scapulae, ribs, a radius and an ulna, were selected to consider both ontogenetic and inter-elemental histological variability (Table 1).

The femur NMQR3282a and tibia NMQR3282b were found together with two lower jaws of similar size in a block of matrix, which allowed these elements to be identified as *Trirachodon*. As these elements were found with two lower jaws, they may either both belong to one individual or they could be from two different individuals (Table 1). The variety of skeletal elements designated as SAM-PK-5881, were

recovered from a bone bed in the Aliwal North district and have all been diagnosed as representing *Trirachodon kannemeyeria*. Several individuals of different sizes were identified, which probably represent different ontogenetic ages. The CGP1/79 radius and ulna belong to a single individual. The largest tibia in the study, SAM-PK-5881c, is designated as adult on the basis of the size and well-finished bone surfaces. This tibia was not directly associated with any other limb bones. Measurements of the complete tibia SAM-PK-5881c were used to estimate the total lengths of the incomplete tibiae. Based on ratios from tibia SAM-PK-5881c, the ratio of diameter to length for the tibiae SAM-PK-5881b and NMQR3282b was calculated. The estimated total length of the tibiae was then divided by the total length of tibia SAM-PK-5881c, and a percentage of adult size was thus obtained (Table 2). Femur NMQR3282a is similar in size to tibia NMQR3282b. Few percentage adult estimations could be calculated as few elements were complete and a fully articulated skeleton of *Trirachodon* was unavailable for study.

As long bones undergo the least secondary remodeling in the midshaft region (Chinsamy 1990, 1991, 1995; Francillon-Vieillot et al. 1990; Horner et al. 1999), all the elements were thin sectioned in this region. The ribs were also sectioned in the midshaft region. As a consequence of their fragmentary nature, only the proximal parts of the scapulae were sectioned. Most of the limb bones were incomplete, but it was possible to thin section the proximal regions of the femur (SAM-PK-5881a) and tibiae (SAM-PK-5881b, SAM-PK-5881c) as well. The thin sectioning technique follows that of Chinsamy and Raath (1992). Terminology used is *sensu* Francillon-Vieillot et al. (1990), Reid (1996), and Starck and Chinsamy (2002).

Several studies have shown that vascularization in bone tissue differs among taxa (Enlow and Brown 1957; Currey 1960; Chinsamy 1991, 1993b) and also among different elements (Horner et al. 2000; Curry 1999; Ray et al. in press). The vascularization of the bone tissue was assessed by mea-

Table 1. The *Trirachodon* specimens examined in this study and their localities. The NMQR3282 elements were found in a matrix that included two similar sized lower jaws. The SAM-PK-5881 elements were recovered from a bone bed in the Aliwal North district and have all been diagnosed as a single species, *Trirachodon kannemeyeria*. They represent several individuals of various sizes and probably stages in ontogenetic age. The CGP1/79 elements belong to a single individual.

District	Specimen number	Skeletal element	Portion sectioned
Kestell	NMQR3282a	femur	midshaft
	NMQR 3282b	tibia	midshaft
Aliwal North	SAM-PK-5881a	femur	midshaft/proximal
	SAM-PK-5881b	tibia	midshaft/proximal
	SAM-PK-5881c	tibia	midshaft/proximal
	SAM-PK-5881d	rib	midshaft
	SAM-PK-5881e	rib	midshaft
	SAM-PK-5881f	scapula	proximal fragments
	SAM-PK-5881g	scapula	proximal fragments
Bergville	CGP1/79a	radius	midshaft
	CGP1/79b	ulna	midshaft

Table 2. Gross measurements of the various *Trirachodon* skeletal elements. Few percentage adult estimations could be calculated as an articulated adult *Trirachodon* specimen was unavailable for comparison.

Specimen number	Skeletal element	Diameter (mm)	Proximal width (mm)	Length (mm)	% Adult
CGP1/79a	radius	3.3	–	40.9	–
CGP1/79b	ulna	5.6	–	40	–
NMQR3282a	femur	5	9	32	51
SAM-PK-5881a	femur	5.5	10	35.2	–
NMQR3282b	tibia	4.8	9.2	32	51
SAM-PK-5881b	tibia	–	13	45.1	72
SAM-PK-5881c	tibia	–	18	62.5	100
SAM-PK-5881d	rib	3.2	–	–	–
SAM-PK-5881e	rib	2.8	–	–	–
SAM-PK-5881f	scapula	3.3	–	–	–
SAM-PK-5881g	scapula	7	–	–	–

suring the area of the channels within the bone (Chinsamy 1993b). However, it should be noted that these channels house not only blood vessels, but also nerves and lymphatic tissue. Calculating the total area of these channels within a given section of bone provides a maximum estimation of vascularization (Chinsamy 1993b; Starck and Chinsamy 2002). These estimations (expressed as percentage channel area) can be compared in different elements, as well as through ontogeny and between different taxa in particular elements.

The cross-sectional geometry method applied in this study measures the relative bone wall thickness (RBT; expressed as a percentage of the diameter) of a transverse thin section of bone (Bühler 1986; Chinsamy 1991). The thickness of the bone wall was measured (in micrometres) at four positions using an eyepiece micrometer in a Nikon Alphaphot-2 YS2 polarizing petrographic microscope at 10X magnification. Two measurements of the bone diameter were also taken in a similar manner. The mean of the four bone wall thickness measurements was divided by the mean bone diameter and the final value expressed as a percentage (RBT) (Fig. 1). The relative bone wall thickness of two thin sections was examined from each midshaft region and the mean was used as the value for the element. Extensive cancellous bone was present in the medullary cavity and thus the relative bone wall thickness in this study refers to the maximum thickness of the compact bone (i.e., excludes cancellous bone).

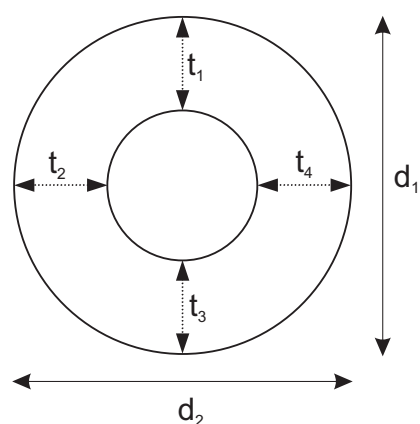
Results

Assessments of developmental stages.—As *Trirachodon* specimens are rare and usually incomplete, it was difficult to obtain gross limb bone measurements for estimating percentage adult sizes of the elements. However, using the nature of the bone tissues, an approximation of ontogenetic development stages was determined. The two lower jaws found in the block of matrix with femur NMQR3282a and tibia

NMQR3282b are similar in size, thus if the femur and tibia (51% adult size) belong to different individuals, they are probably of similar ontogenetic age. The tibia SAM-PK-5881b was calculated to be approximately 72% of the adult size.

Bone histology analysis.—A comprehensive assessment of *Trirachodon* postcranial elements characteristically showed zonal bone tissue. In all the elements the zones consist of moderately vascularized fibro-lamellar tissue, alternating with either poorly vascularized annuli or lines of arrested growth (LAGs).

The bone wall thickness of femur NMQR3282a is 29% that of the diameter of the bone (i.e., 29% RBT). The bone appears highly vascularized and the percentage area occupied by the channels in the bone is 10.8%. The fibro-lamellar bone tissue is interrupted by two narrow incomplete annuli (Fig. 2A). Numerous primary osteons are obliquely oriented to form a reticular network and the osteocyte lacunae are globular and



$$D (\text{diameter}) = (d_1 + d_2)/2$$

$$T (\text{cortical thickness}) = (t_1 + t_2 + t_3 + t_4)/4$$

$$(\text{RBT}) = (T/D) \times 100$$

Fig. 1. Schematic representation of the relative bone wall thickness (RBT) measurements, expressed as a percentage (modified from Chinsamy 1991).

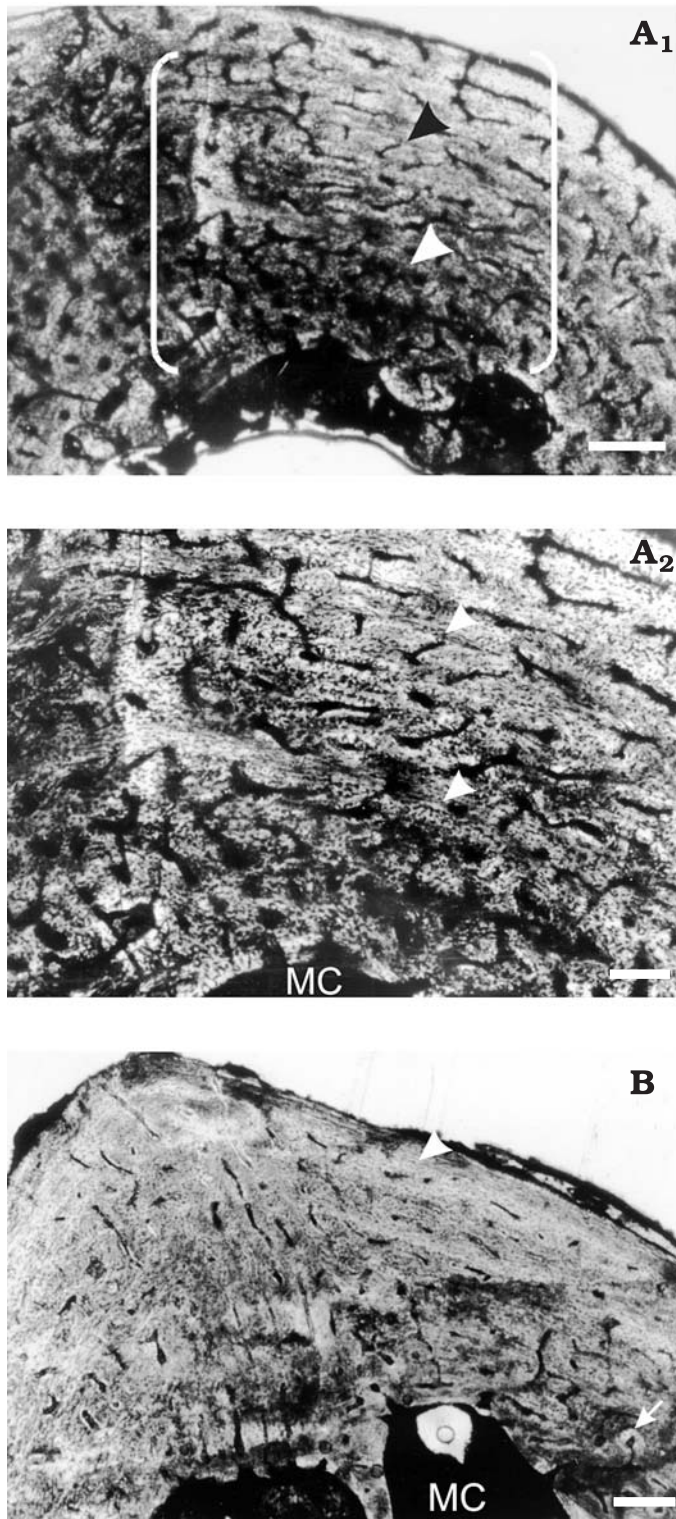


Fig. 2. Transverse sections of *Trirachodon* femora. A. Femur (NMQR3282a), estimated to be 51% adult size; A₁, highly vascularized fibro-lamellar bone, scale bar 250 µm; A₂, high magnification of the same, showing two indistinct annuli (arrowheads), scale bar 125 µm. B. Femur (SAM-PK-5881a) consisting of moderately vascularized fibro-lamellar bone with a parallel-fibred region at the periphery (arrowhead). The vascular canals are radially and longitudinally orientated, with some anastomoses. Arrow indicates a secondary osteon, scale bar 250 µm. MC indicates medullary cavity.

radiate branched canaliculi. The inner annulus forms an almost complete circle, disappearing on the ventro-medial side, and the outer annulus disappears on the dorso-lateral and ventro-medial sides of the bone. The osteocyte lacunae in the annuli are better organized in these regions, which makes the annuli more easily discernable from the rest of the cortical tissue. Vascularization does not decrease at the periphery and some secondary remodeling is present.

Thin sections were taken slightly proximal to the middle of the midshaft region of femur SAM-PK-5881a. The bone tissue (31% RBT) consists of fibro-lamellar tissue (Fig. 2B), which is less vascularized (% channel area = 4.5%) than femur NMQR3282a. In the fibro-lamellar bone, the osteocyte lacunae are similar to those of femur NMQR3282a described above, but they tend to become more organized in parallel-fibred bone tissue, at the periphery of the bone. In more proximal sections, small secondary osteons are seen around the medullary cavity. Bone drift occurs in the region of the lesser trochanter, where remodeled tissue, in the form of compacted coarse cancellous bone, almost reaches the sub-periosteal surface. The dorsal and lateral sides of the bones contain more compact tissue than the ventral and medial regions.

The organization of bone in the tibia NMQR3282b (25% RBT) is similar to that described for femur NMQR3282a. The highly vascularized tissue (% channel area = 11.4%) forms a reticular network and is interrupted by two narrow poorly defined annuli, similar to femur NMQR3282a (Fig. 3A).

Longitudinally oriented primary osteons dominate the tissues of the tibiae SAM-PK-5881b and SAM-PK-5881c (% channel area = 4.2%). The bone tissue is interrupted by annuli, which are sometimes associated with LAGs (Fig. 3B). The globular osteocyte lacunae have radiating canaliculi, as in the other elements described above. Secondary osteons are distributed throughout the cortex in both elements. The more proximal sections of SAM-PK-5881b show extreme secondary remodeling which reaches a parallel-fibred region at the periphery of the bone. Extensive secondary remodeling was noted on the medial side of SAM-PK-5881c in the proximal metaphyseal region.

The bone tissue of the scapulae SAM-PK-5881f and SAM-PK-5881g consists of fibro-lamellar tissue alternating with annuli (Fig. 4A). The annuli are more prominent in the smaller scapula (SAM-PK-5881f). One annulus can be seen towards the sub-periosteal surface of SAM-PK-5881g (Fig. 4A). Longitudinally oriented primary osteons dominate in SAM-PK-5881f, whereas circumferential anastomoses are associated with the vascular canals in SAM-PK-5881g. A slight decrease in vascularization occurs at the periphery of SAM-PK-5881g. Secondary osteons are observed scattered throughout the cortex in SAM-PK-5881f, but are more abundant in the peri-medullary region. Large resorption cavities in the peri-medullary regions of both elements are observed.

The ribs SAM-PK-5881d and SAM-PK-5881e consist of moderately vascularized fibro-lamellar bone interrupted occasionally by LAGs, which are sometimes multiple (Fig. 4B).

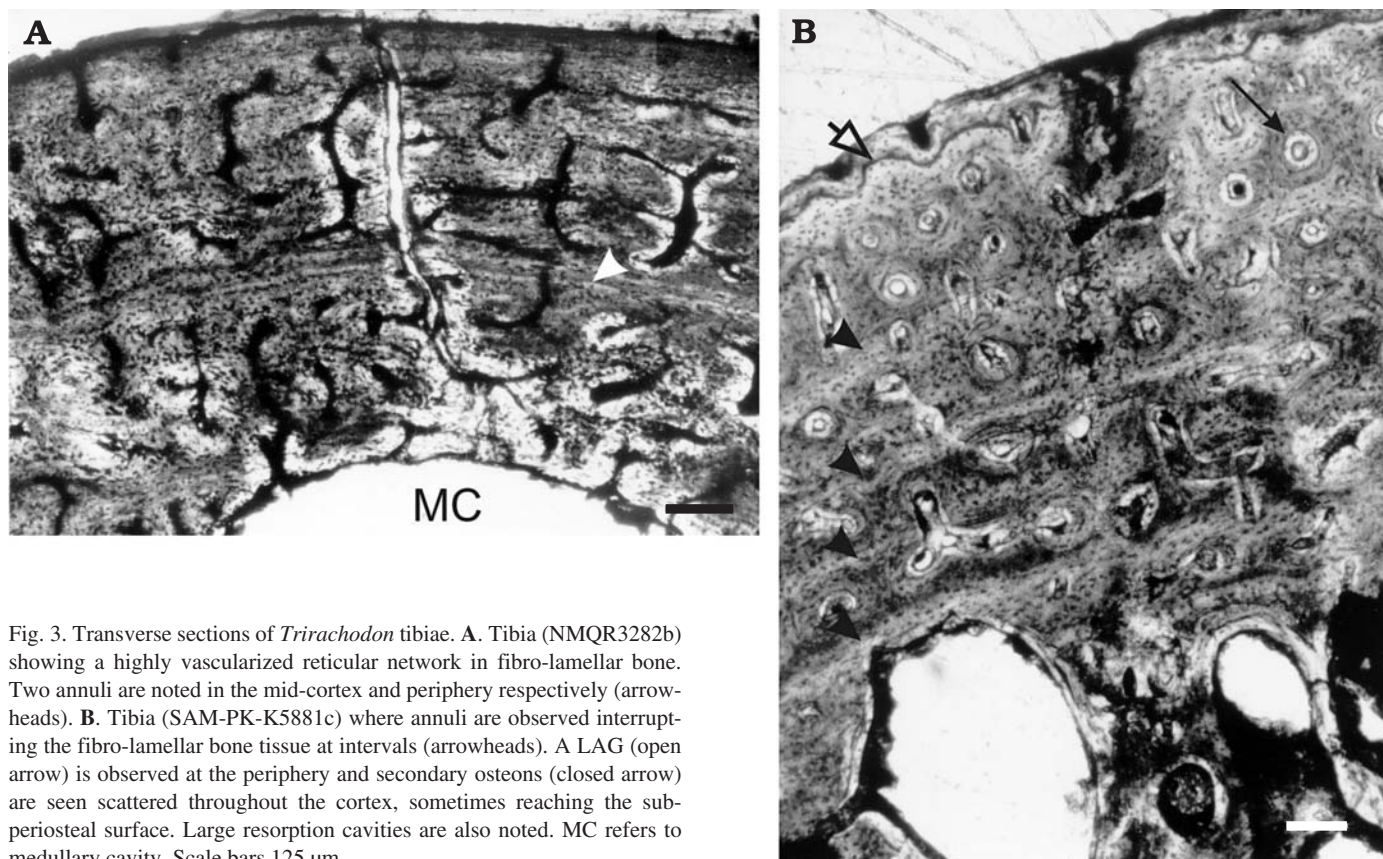


Fig. 3. Transverse sections of *Trirachodon* tibiae. **A.** Tibia (NMQR3282b) showing a highly vascularized reticular network in fibro-lamellar bone. Two annuli are noted in the mid-cortex and periphery respectively (arrowheads). **B.** Tibia (SAM-PK-K5881c) where annuli are observed interrupting the fibro-lamellar bone tissue at intervals (arrowheads). A LAG (open arrow) is observed at the periphery and secondary osteons (closed arrow) are seen scattered throughout the cortex, sometimes reaching the sub-periosteal surface. Large resorption cavities are also noted. MC refers to medullary cavity. Scale bars 125 μ m.

The vascular canals vary from radially arranged canals to longitudinally oriented primary osteons, becoming slightly more scarce towards the periphery. Secondary osteons are common and may reach the outer cortex in some areas, but are more abundant around the medullary cavity. Erosionally enlarged resorption cavities are observed in the peri-medullary regions.

The bone tissue of the radius CGP1/79a (26% RBT) consists of moderately vascularized (% channel area = 4%) fibro-lamellar tissue, which becomes less vascularized and more organized towards the periphery. Closely spaced annuli, consisting of parallel-fibred bone, and a LAG can be seen at the periphery of the bone (Fig. 5A). Vascularization varies from longitudinally oriented primary osteons with occasional radial anastomoses, to radially oriented canals. As in the femora, the osteocyte lacunae tend to be globular and a few small secondary osteons are recognized in the peri-medullary region.

The ulna CGP1/79b, which is from the same individual as radius CGP1/79a (25% RBT), exhibits zonal bone tissue, consisting of moderately vascularized (% channel area = 3.7%) fibro-lamellar tissue, interrupted by poorly vascularized bands of annuli that comprise lamellar tissue (Fig. 5B). Vascularization is mostly in the form of longitudinally oriented primary osteons. The osteocyte lacunae are similar to those of the radius and several small secondary osteons are present in the peri-medullary region. Sharpey's fibers are located in the region of the ulna crest.

Discussion

The fibro-lamellar tissue and abundant vascular canals in the femur NMQR3282a (% channel area = 10.8%) and tibia NMQR3282b (% channel area = 11.4%) suggest rapid rates of bone deposition and hence growth. Fibro-lamellar bone is recognized as having a faster deposition rate compared to other types of bone tissue organizations (Amprino 1947; Francillon-Vieillot et al. 1990; Margerie et al. 2002). The presence and abundance of primary osteons is related to fast growth, although the particular orientation of the vascular canals (in this case reticular) is not necessarily connected to growth rate (Margerie et al. 2002). Vascularization remains constant throughout the cortex in both the femur and tibia. The nature of the bone "vascularization" suggests that bone deposition and hence appositional growth was still occurring at a rapid rate at the time of death, which implies that these skeletal elements were from an immature individual/s.

The total length of femur SAM-PK-5881a (32 mm) almost equals that of femur NMQR3282a (35.2 mm), but the channel area of femur SAM-PK-5881a (4.5%) is markedly lower than that of femur NMQR3282a (10.8%). The low percentage channel area combined with the parallel-fibred bone at the sub-periosteal surface suggests that SAM-PK-5881a represents a more mature individual than femur NMQR3282a, even though the bones are of similar length. If the change in bone

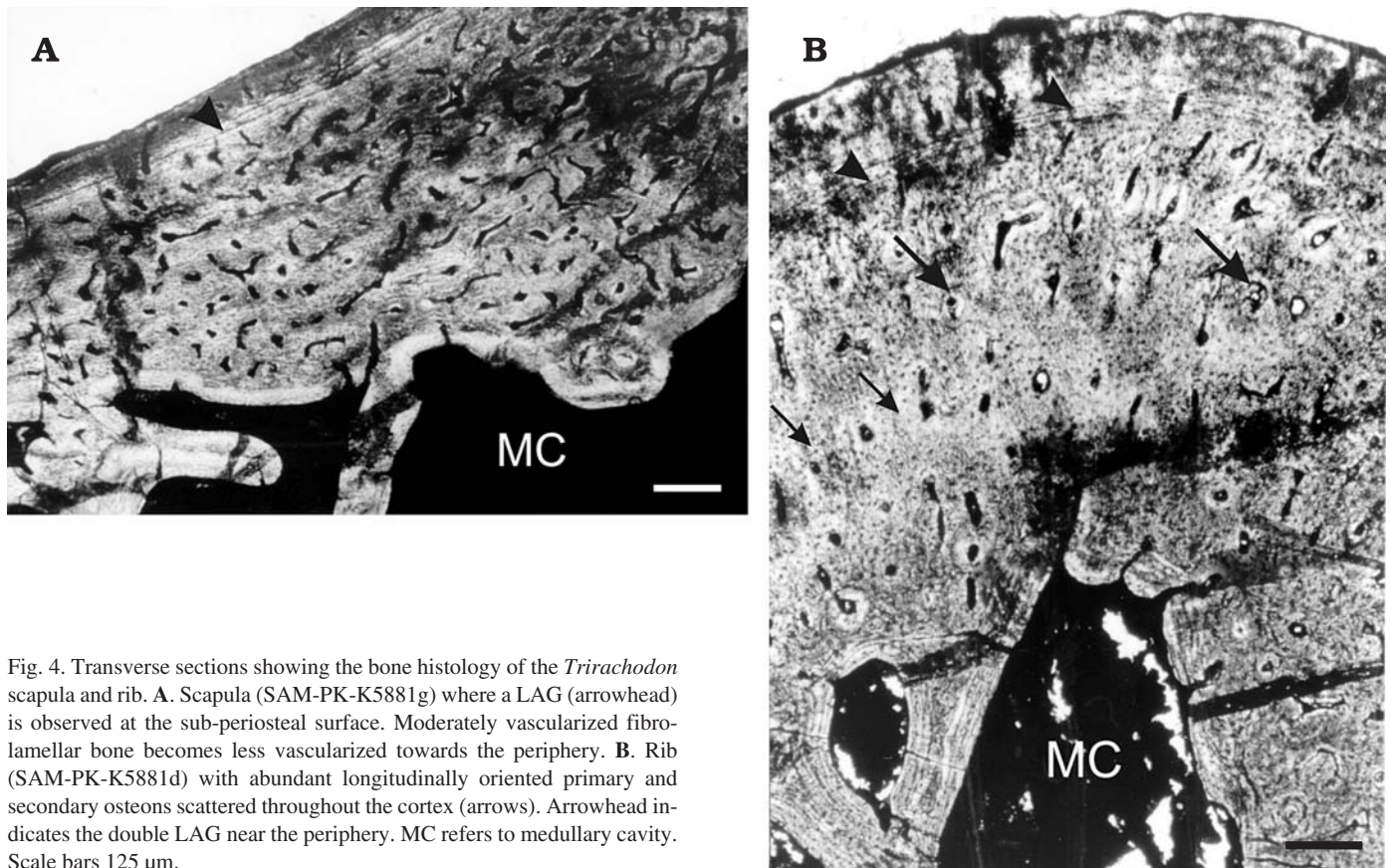


Fig. 4. Transverse sections showing the bone histology of the *Trirachodon* scapula and rib. **A.** Scapula (SAM-PK-K5881g) where a LAG (arrowhead) is observed at the sub-periosteal surface. Moderately vascularized fibrolamellar bone becomes less vascularized towards the periphery. **B.** Rib (SAM-PK-K5881d) with abundant longitudinally oriented primary and secondary osteons scattered throughout the cortex (arrows). Arrowhead indicates the double LAG near the periphery. MC refers to medullary cavity. Scale bars 125 μ m.

tissue represents a permanent change to parallel-fibred bone, then the overall growth rate had probably begun to slow. An alternative explanation could be that the parallel-fibred region in femur SAM-PK-5881a may be an annulus, representing only a temporary decrease in growth rate. The notable difference in vascularization between these two femora may be due to individual variation, gender or taxonomic differences. It is unlikely to be the results of local histological variation within the femur as the image analysis was conducted on sections taken from the midshaft regions in both elements. The difference in percentage channel area (i.e., % "vascularization") may be due to individual variation as the bones are from different individuals and different localities. It is also possible that these elements are from different *Trirachodon* species. The NMQR3282 material was collected from Kestell and has only been identified to genus level. As a result, the material may represent any of the three morphospecies described by Rubidge and Sidor (2001). In contrast, the SAM-PK material was collected from Aliwal North and has been identified as *Trirachodon kannemeyeria*.

Tibia SAM-PK-K5881c is the largest element in the study and has been designated an adult due to its large size, whereas tibia NMQR3282b is approximately 50% of the length of tibia SAM-PK-5881c. The tibiae SAM-PK-K5881b and SAM-PK-5881c have more abundant and well-defined annuli and LAGs, and secondary remodeling is more extensive in these elements compared to tibia NMQR3282b. This suggests that

tibia SAM-PK-5881b and SAM-PK-5881c are ontogenetically older than tibia NMQR3282b. The vascularization of tibia SAM-PK-5881c (4.2%) is distinctly lower than that of tibia, NMQR3282b (11.4%). The channel area of tibia SAM-PK-5881b could not be quantified due to poor preservation, but it is moderately vascularized and appears similar to tibia SAM-PK-5881c. Thus, the decrease in vascularization indicates that overall growth slowed with age.

The slight decrease in vascularization at the sub-periosteal surface of scapula SAM-PK-5881g suggests that growth in this element had begun to slow down. The scapula SAM-PK-5881f is moderately vascularized and there is no decrease in vascularization at the periphery. The absence of any decrease in vascularization, combined with the smaller diameter suggests that SAM-PK-5881f is ontogenetically younger than SAM-PK-5881g (3.3 mm and 7 mm diameter respectively). The prominent, sometimes multiple LAGs in the ribs suggest that they experienced several periods of pauses in growth, which may have been in response to particularly harsh seasons, or perhaps inherent slow growth in the ribs.

The radius CGP1/79a and ulna CGP1/79b are from a single individual. The decrease in vascularization towards the periphery of the radius suggests that this individual had reached maturity. The relatively low percentage channel area of both elements (radius 4%, ulna 3.7%) supports this suggestion. Growth rings are present in both elements and indicate a periodic decrease in bone deposition, and hence growth.

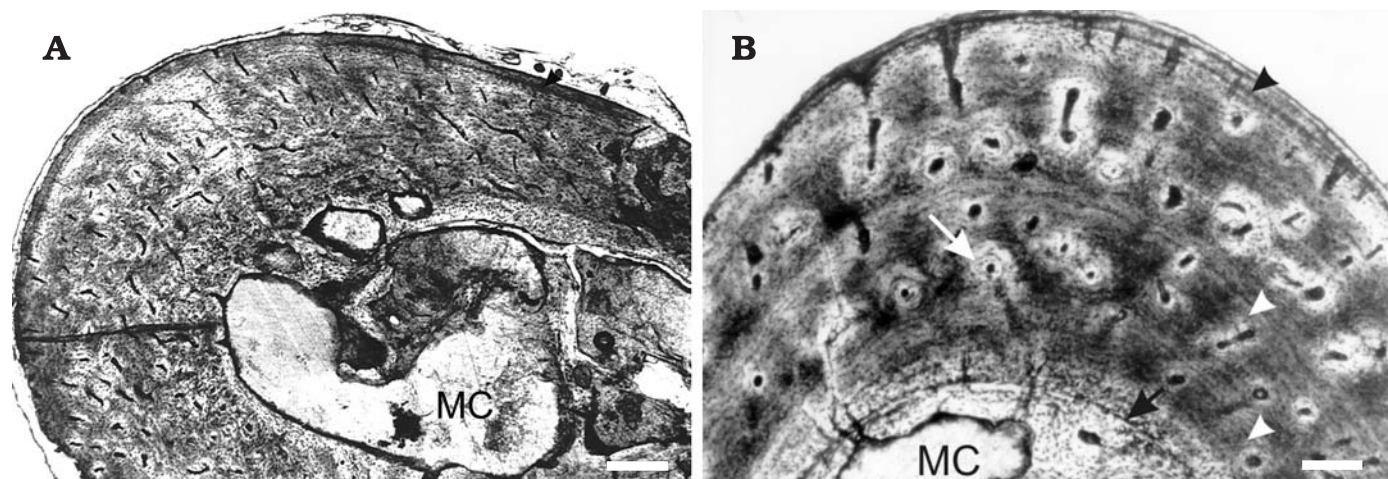


Fig. 5. The bone histology of a *Trirachodon* radius and ulna, from a single individual (CGP1/79). **A.** Radius (CGP1/79a), note the annuli containing parallel-fibered tissue and the LAG at the periphery of the bone (arrowhead). Vascularization decreases towards the periphery. Remodeling has occurred as is evident from the resorption cavities in the peri-medullary cavity. Scale bar 250 μ m. **B.** Ulna (CGP1/79b), the tissue consists of moderately vascularized fibro-lamellar tissue, which is interrupted by annuli (arrowheads). Secondary osteons are scattered throughout the cortex (white arrow). MC indicates medullary cavity. Scale bar 125 μ m.

Growth patterns.—The predominance of fibro-lamellar bone tissue in *Trirachodon* suggests an overall rapid growth rate. The presence of growth rings in all the elements studied, however, indicates that *Trirachodon* experienced periodic interruptions in this fast growth rate. The annuli indicate that growth slowed down during the unfavourable growing period, or even ceased temporarily, as indicated by LAGs, in older individuals (as seen in tibiae SAM-PK-5881b and SAM-PK-5881c). *Trirachodon* is found in deposits with ephemeral stream sandstones, which suggest that the local climate was semi-arid with a seasonal rainfall (Smith et al. 1993). Studies on extant animals have shown that zones are deposited during the favourable growing season and annuli and/or LAGs during the unfavourable growing season (Hutton 1986; Reid 1990). Thus, such features in *Trirachodon* suggest that its growth rate could have been influenced by seasonal fluctuations.

Comparison of *Trirachodon* with contemporary non-mammalian cynodonts.—*Diademodon*, a large, omnivorous derived non-mammalian cynodont that was contemporary with *Trirachodon* shows a similar bone tissue pattern to that of *Trirachodon* (Botha and Chinsamy 2000). This suggests that both *Trirachodon* and *Diademodon* were affected by environmental conditions. There are some differences between the two genera, however, as growth cycles are more distinct in the *Diademodon* samples studied as compared to those of *Trirachodon*, a difference suggesting that *Trirachodon* was perhaps slightly less susceptible to seasonal variation than was *Diademodon*. The bone tissue of *Trirachodon* also appears similar to that of the Middle Triassic *Gomphodontosuchus* from Brazil, which exhibits an alternating pattern of fast and slow growth (Ricqlès 1969).

In contrast, the bone histology of *Cynognathus*, a large, carnivorous, derived non-mammalian cynodont, differs considerably from that of *Trirachodon* and *Diademodon* in that

here the bone consists of highly vascularized, uninterrupted fibro-lamellar tissue (Botha and Chinsamy 2000). The bone tissue of *Cynognathus* appears similar to that of the Middle Triassic Brazilian insectivorous *Belesodon* and herbivorous *Traversodon* (Ricqlès 1969). These findings suggest that *Cynognathus* (Botha and Chinsamy 2000), *Belesodon* and *Traversodon* (Ricqlès 1969) growth was less susceptible to ambient conditions as compared to *Trirachodon*, *Diademodon* (Botha and Chinsamy 2000), and *Gomphodontosuchus* (Ricqlès 1969).

Inter-elemental histovariability.—Although the percentage channel area does not vary significantly among the different limb bones, slight variations in bone tissue organization were noted. All the bones exhibit zonal bone tissue, but the number and extent of annuli and LAGs differ among the various elements and only the tibiae, ulnae and ribs exhibited multiple LAGs. It is possible that these bones were ontogenetically older than the other elements and grew more slowly, thus exhibiting multiple LAGs. The ulna (CGP1/79a) and radius (CGP1/79b) belong to the same individual, and although the ulna exhibits multiple LAGs, the radius does not. The latter, however, has extensive endosteal resorption, which may have removed earlier growth cycles. Thus, it is evident that the ulna and radius experienced different remodeling processes, and it is likely that they also had differential growth rates.

Lifestyle adaptations.—It is well-known that adaptations to an amphibious or aquatic lifestyle often lead to a high RBT (e.g., Wall 1983; Bou et al. 1990; Chinsamy 1997). However, it appears that a burrowing/fossorial lifestyle also results in thick bone walls (i.e., high RBT). The femur of the naked mole rat (*Heterocephalus glaber*), which lives in extensive burrow complexes, has a similar RBT to *Trirachodon* of 31%. Similarly, Magwene (1993) found that the burrowing or digging lizards *Gerrhonotus grantis*, *Heloderma sus-*

pectum, and *Phrynosoma douglassi* as well as the new world porcupine *Erethizon*, which is known to burrow, have a femoral RBT exceeding 30%. In contrast, the femoral RBT values of non-fossorial extant lizards such as *Varanus arenarius*, *Varanus nuchalis* (monitor lizards) and *Iguana tuberculata* (iguana lizard) range from 15.5% to 19%, and those of the non-fossorial mammals *Erinaceus* (hedgehog), *Viverra* (civet) and *Lepus* (hare) range from 17.4% to 23% (Magwene 1993). This pattern suggests that digging or burrowing animals have higher RBT values (usually more than 30%) than non-fossorial animals (less than 30%).

The average femoral RBT value for *Trirachodon* is 30%. As there are no morphological adaptations to indicate that *Trirachodon* was aquatic or semi-aquatic (Kemp 1982), it is more likely that it was fossorial. This hypothesis is supported by the fact that *Trirachodon* skeletons encased in calcareous nodules, identified as terminal chambers, have been found associated with a burrow complex from the Early Triassic Driekoppen Formation of South Africa (Groenewald et al. 2001), and *Trirachodon* skeletons, associated with burrows, have also been recovered from a Mid-Triassic rift valley fill in the Omingonde Formation of Central Namibia (Smith and Swart 2002). Thus, it is likely that *Trirachodon* used its relatively thick limb bones to maneuver through and dig its burrow system (Bou et al. 1990; Casinos et al. 1993), perhaps to escape harsh climatic conditions as suggested for *Diictodon* (Smith 1987; Ray and Chinsamy 2004).

Conclusions

This study provides insight into the growth patterns and life-style adaptations of *Trirachodon* using bone histology and limb bone cross-sectional geometry. The bone histology reveals moderately vascularized, fibro-lamellar bone alternating with annuli or LAGs. Some inter-elemental histovariability was observed in that the number and extent of growth rings varied. Similar regions of the bones were compared when interpreting growth patterns, as bone histological interpretations of a single element may differ depending on which region of the element is analysed. Palaeoenvironmental evidence suggests that the environment was semi-arid with seasonal rainfall, and as all the study elements exhibit zonal bone, it is possible that *Trirachodon* was affected by such environmental fluctuations. Thus, overall growth was rapid, but slowed down or ceased temporarily, possibly during the unfavourable growing season. The bone cross-sectional geometry results in this study support earlier proposals that *Trirachodon* was fossorial and may have burrowed to escape harsh environmental conditions.

Acknowledgements

The following individuals are thanked for the loan of the study material: Roger Smith and Derek Ohland of the Natural History Division,

Iziko Museums of Cape Town, Johann Welman, previously of the National Museum, Bloemfontein, and Johann Neveling of the Council for Geoscience, Pretoria. This work was supported by the National Research Foundation under Grant Number 2047145.

References

- Amprino, R. 1947. La structure du tissu osseux envisagée comme expression de différences dans la vitesse de l'accroissement. *Archives de Biologie* 58: 315–330.
- Botha, J. and Chinsamy, A. 2000. Growth patterns from the bone histology of the cynodonts *Diademodon* and *Cynognathus*. *Journal of Vertebrate Paleontology* 20: 705–711.
- Bou, J., Castiella, M.J., Ocana, J., and Casinos, A. 1990. Multivariate analysis and locomotor morphology in insectivores and rodents. *Zoologischer Anzeiger* 225: 287–294.
- Bühler, P. 1986. Das Vogelskelet-hochentwickelter Knochen-leichtbau. *Arcus* 5: 221–228.
- Carrier, D.R. 1987. The evolution of locomotor stamina in tetrapods: Circumventing a mechanical constraint. *Paleobiology* 13: 326–341.
- Casinos, A., Quintana, C., and Viladiu, C. 1993. Allometry and adaptation in the long bones of a digging group of rodents (Ctenomyiinae). *Zoological Journal of the Linnean Society* 107: 107–115.
- Chinsamy, A. 1990. Physiological implications of the bone histology of *Syntarsus rhodesiensis* (Saurischia: Theropoda). *Palaeontologia Africana* 27: 77–82.
- Chinsamy, A. 1991. *The Osteohistology of Femoral Growth within a Clade: A Comparison of the Crocodile Crocodylus, the Dinosaurs Massospondylus and Syntarsus, and the Birds Struthio and Sagittarius*. 200 pp. Ph.D. dissertation, University of Witwatersrand, Johannesburg.
- Chinsamy, A. 1993a. Bone histology and growth trajectory of the prosauropod dinosaur *Massospondylus carinatus* Owen. *Modern Geology* 18: 319–329.
- Chinsamy, A. 1993b. Image analysis and the physiological implications of the vascularisation of femora in archosaurs. *Modern Geology* 19: 101–108.
- Chinsamy, A. 1995. Ontogenetic changes in the bone histology of the Late Jurassic ornithomimid *Dryosaurus lettowvorbecki*. *Journal of Vertebrate Paleontology* 15 (1): 96–104.
- Chinsamy, A. 1997. Assessing the biology of fossil vertebrates through bone histology. *Palaeontologia Africana* 33: 29–35.
- Chinsamy, A. and Raath, M.A. 1992. Preparation of fossil bone for histological examination. *Palaeontologia Africana* 29: 39–44.
- Crompton, A.W. and Ellenberger, F. 1957. On a new cynodont from Molteno Beds and origin of tritylodontids. *Annals of the South African Museum* 44: 1–14.
- Currey, J.D. 1960. Differences in the blood-supply of bone of different histological types. *Quarterly Journal of Microscopical Science* 101 (3): 351–370.
- Curry, K.A. 1999. Ontogenetic histology of *Apatosaurus* (Dinosauria: Sauropoda): New insights on growth rates and longevity. *Journal of Vertebrate Paleontology* 19 (4): 654–665.
- Enlow, D.H. and Brown, S.O. 1956. A comparative histological study of fossil and recent bone tissues. Part I. *The Texas Journal of Science* 8: 405–443.
- Enlow, D.H. and Brown, S.O. 1957. A comparative histological study of fossil and recent bone tissues. Part II. *The Texas Journal of Science* 9: 136–214.
- Fish, F.E. 1993. Comparison of swimming kinematics between terrestrial and semiaquatic opossums. *Journal of Mammalogy* 74 (2): 275–284.
- Francillon-Vieillot, H., de Buffrénil, V., Castanet, J., Geraudie, J., Meunier, F.J., Sire, J.Y., Zylberberg, L., and de Ricqlès, A. 1990. Microstructure and mineralization of vertebrate skeletal tissues. In: J.G. Carter (ed.), *Skeletal Biomineralization: Patterns, Processes and Evolutionary Trends*, 471–548. Van Nostrand Reinhold, New York.

- Groenewald, G.H., Welman, J., and MacEachern, J.A. 2001. Vertebrate burrow complexes from the Early Triassic *Cynognathus* Zone (Driekoppen Formation, Beaufort Group) of the Karoo Basin, South Africa. *Palaios* 16: 148–160.
- Horner, J.R., de Ricqlès, A., and Padian, K. 1999. Variation in dinosaur skeletochronology indicators: Implications for age assessment and physiology. *Paleobiology* 25: 295–304.
- Horner, J.R., de Ricqlès, A., and Padian, K. 2000. Long bone histology of the hadrosaurid dinosaur *Maiasaura peeblesorum*: Growth dynamics and physiology of an ontogenetic series of skeletal elements. *Journal of Vertebrate Paleontology* 20: 115–129.
- Hutton, J.M. 1986. Age determination of living Nile crocodiles from the cortical stratification of bone. *Copeia* 2: 332–341.
- Kemp, T.S. 1982. *Mammal-like Reptiles and the Origin of Mammals*. 363 pp. Academic Press, London.
- Magwene, P.M. 1993. *What's Bred in the Bone: Histology and Cross-sectional Geometry of Mammal-like Reptile Long Bones—Evidence of Changing Physiological and Biomechanical Demands*. 54 pp. M.Sc. dissertation, Harvard University, Cambridge.
- Margerie, E. de, Cubo, J., and Castanet, J. 2002. Bone typology and growth rate: testing and quantifying “Amprino’s rule” in the mallard (*Anas platyrhynchos*). *Comptes Rendus Biologies* 325: 221–230.
- Pough, F.H., Heiser, J.B., and McFarland, W.N. 1996. *Vertebrate Life*. 798 pp. Prentice-Hall, New Jersey.
- Ray, S. and Chinsamy, A. 2004. *Diictodon feliceps* (Therapsida, Dicynodontia): bone histology, growth and biomechanics. *Journal of Vertebrate Paleontology* 24: 180–194.
- Ray, S., Botha, J., and Chinsamy, A. (in press). Bone histology and growth patterns of some nonmammalian therapsids. *Journal of Vertebrate Paleontology*.
- Reid, R.E.H. 1990. Zonal “growth rings” in dinosaurs. *Modern Geology* 15: 19–48.
- Reid, R.E.H. 1996. Bone histology of the Cleveland-Lloyd dinosaurs and of dinosaurs in general, Part I: Introduction: Introduction to bone tissues. *Geology Studies* 41: 25–71.
- Ricqlès, A., de 1969. Recherches paléohistologiques sur les os longs des tétrapodes. II. – Quelques observations sur la structure des os longs des Thérodontes. *Annales de Paléontologie (Vertebres)* 55 (1): 1–52.
- Ricqlès, A., de 1972. Recherches paléohistologiques sur les os longs des tétrapodes. III. – Titanosuchiens, Dinocéphales et Dicynodontes. *Annales de Paléontologie (Vertebres)* 58 (1): 17–60.
- Ricqlès, A., de 1974. Evolution of endothermy: Histological evidence. *Evolutionary Theory* 1: 51–80.
- Ricqlès, A., de 1976. On bone histology of fossil and living reptiles, with comments on its functional and evolutionary significance. In: A. d’A. Bellairs and C.B. Cox (eds.), *Morphology and Biology of Reptiles*, 123–150. Academic Press, London.
- Ricqlès, A., de 1980. (ed.) Tissue structures of dinosaur bone. Functional significance and possible relation to dinosaur physiology. In: D.K. Thomas and E.C. Olson (eds.), *A Cold Look at the Warm-blooded Dinosaurs*, 103–139. Westview Press, Boulder.
- Ricqlès, A., de, Padian, K., and Horner, J.R. 2001. The bone histology of basal birds in phylogenetic and ontogenetic perspectives. In: J. Gauthier and L.F. Gall (eds.), *New Perspectives on the Origin and Early Evolution of Birds: Proceedings of the International Symposium in Honor of John H. Ostrom*, 411–426. Peabody Museum of Natural History, New Haven.
- Ricqlès, A., de, Padian, K., Horner, J.R., Lamm, E.-T., and Myhrvold, N. 2003. Osteohistology of *Confuciusornis sanctus* (Theropoda: Aves). *Journal of Vertebrate Paleontology* 23: 373–386.
- Rubidge, B.S. (ed.) 1995. *Biostratigraphy of the Beaufort Group (Karoo Supergroup)*. 46 pp. Council for Geoscience, Pretoria.
- Rubidge, B.S. and Sidor, C.A. 2001. Evolutionary patterns among Permian-Triassic therapsids. *Annual Review of Ecology and Systematics* 32: 449–480.
- Seeley, H.G. 1895a. Researches on the structure, organization and classification of the fossil Reptilia. On *Diademdon*. *Philosophical Transactions of the Royal Society of London B* 185: 1029–1041.
- Seeley, H.G. 1895b. On the structure, organization and classification of the fossil Reptilia III. On *Trirachodon*. *Philosophical Transactions of the Royal Society of London B* 186: 48–57.
- Smith, R. 1987. Helical burrow casts of therapsid origin from the Beaufort Group (Permian) of South Africa. *Palaeogeography, Palaeoclimatology, Palaeoecology* 60: 155–170.
- Smith, R. and Swart, R. 2002. Changing fluvial environments and vertebrate taphonomy in response to climatic drying in a Mid-Triassic rift valley fill: The Omingonde Formation (Karoo Supergroup) of Central Namibia. *Palaos* 17 (3): 249–267.
- Starck, J.M. and Chinsamy, A. 2002. Bone microstructure and developmental plasticity in birds and other dinosaurs. *Journal of Morphology* 254: 232–246.
- Stein, B.R. 1989. Bone density and adaptation in semi-aquatic mammals. *Journal of Mammalogy* 70 (3): 467–476.
- Wall, W.P. 1983. The correlation between limb-bone density and aquatic habits in recent mammals. *Journal of Vertebrate Paleontology* 57: 197–207.